Toxicology and Applied Pharmacology 470 (2023) 116548

Contents lists available at ScienceDirect

Toxicology and Applied Pharmacology

journal homepage: www.elsevier.com/locate/taap

Focusing on the 5F-MDMB-PICA, 4F-MDMB-BICA synthetic cannabinoids and their primary metabolites in analytical and pharmacological aspects

Szabolcs Dvorácskó [a,b], Tímea Körmöczi [c], Éva Sija [d], Balázs Bende [e], Roland Weiczner [d], Tibor Varga [f], István Ilisz [c], László Institóris [d], Éva M. Kereszty [d], Csaba Tömböly [a], Róbert Berkecz [c,*]

[a] Laboratory of Chemical Biology, Institute of Biochemistry, Biological Research Centre, Temesvári krt. 62, Szeged, Hungary
[b] Department of Medical Chemistry, Albert Szent-Györgyi Medical School, University of Szeged, Dóm tér 8, Szeged, Hungary
[c] Institute of Pharmaceutical Analysis, Faculty of Pharmacy, University of Szeged Somogyi, utca 4., Szeged, Hungary
[d] Department of Forensic Medicine, Albert Szent-Györgyi Health Centre, Kossuth Lajos sgt. 40., Szeged, Hungary
[e] Department of Dermatology and Allergology, Albert Szent-Györgyi Health Center, H-6720 Szeged, Korányi fasor 6., Szeged, Hungary
[f] Drug Laboratory Szeged, Drug Investigation Department, Hungarian Institute for Forensic Sciences, Kossuth Lajos sgt. 22-24, Szeged, Hungary

ARTICLE INFO

Editor: Lawrence Lash

Keywords:
Synthetic cannabinoids
Main metabolites
UHPLC-MS/MS
CB1R binding affinities
Polydrug use

ABSTRACT

Nowadays, more and more new synthetic cannabinoids (SCs) appearing on the illicit market present challenges to analytical, forensic, and toxicology experts. For a better understanding of the physiological effect of SCs, the key issue is studying their metabolomic and psychoactive properties.

In this study, our validated targeted reversed phase UHPLC-MS/MS method was used for determination of urinary concentration of 5F-MDMB-PICA, 4F-MDMB-BICA, and their primary metabolites. The liquid-liquid extraction procedure was applied for the enrichment of SCs. The pharmacological characterization of investigated SCs were studied by radioligand competition binding and ligand stimulated [^{35}S]GTPγS binding assays.

For 5F-MDMB-PICA and 4F-MDMB-BICA, the median urinary concentrations were 0.076 and 0.312 ng/mL. For primary metabolites, the concentration range was 0.029–881.02* ng/mL for 5F-MDMB-PICA-COOH, and 0.396–4579* ng/mL for 4F-MDMB-BICA-COOH. In the polydrug aspect, the 22 urine samples were verified to be abused with 6 illicit drugs. The affinity of the metabolites to CB1R significantly decreased compared to the parent ligands. In the GTPγS functional assay, both 5F-MDMB-PICA and 4F-MDMB-BICA were acting as full agonists, while the metabolites were found as weak inverse agonists. Additionally, the G-protein stimulatory effects of the full agonist 5F-MDMB-PICA and 4F-MDMB-BICA were reduced by metabolites. These results strongly indicate the dose-dependent CB1R-mediated weak inverse agonist effects of the two butanoic acid metabolites.

The obtained high concentration of main urinary metabolites of 5F-MDMB-PICA and 4F-MDMB-BICA confirmed the relevance of their routine analysis in forensic and toxicological practices. Based on *in vitro* binding assays, the metabolites presumably might cause a lower psychoactive effect than parent compounds.

1. Introduction

The emergence of new psychoactive substances (NPS) such as cathinones, synthetic cannabinoids (SCs), phenethylamines, opioids, tryptamines, benzodiazepines, piperazines, etc. has been associated with high health and social risk globally since 2008 (Luethi and Liechti, 2020). Nowadays, the SCs have been one of the main representatives of NPS and their rapid appearance and relatively short presence on the global drug market pose great challenges in drug-related political, forensic, toxicological, and analytical aspects. In order to circumvent the applicable drug law, the combination of the structural units (core, tails, andlinkers) of SCs provides the opportunity for the synthesis of newer and newer SC representatives having presumed psychoactive properties, and they will appear as "legal high" products on the drug market (Potts et al., 2020; Angerer et al., 2018). These "developments" trigger the continuous updating of related analytical methods, toxicological, and pharmacological data having been essential in recent days.

The 5F-MDMB-PICA as a ingredient of "spice-like" herbal incenses

* Corresponding author.
E-mail address: berkecz.robert@szte.hu (R. Berkecz).

https://doi.org/10.1016/j.taap.2023.116548
Received 16 December 2022; Received in revised form 2 May 2023; Accepted 7 May 2023
Available online 12 May 2023

was first described in 2017 (Risseeuw et al., 2017). In that year, twelve phase I and two phase II metabolites of 5F-MDMB-PICA were characterized and the ester hydrolysis and mono-hydroxylation (at indole ring) urinary metabolites were selected as targets for proof of its consumption (Mogler et al., 2018; Qin et al., 2022). Several intoxications and lethal outcomes were reported related with the consumption of 5F-MDMB-PICA (Brandt, 2019; Kleis et al., 2020; Musa et al., 2020; Shi et al., 2020). The 4F-MDMB-BICA, as one of the newest SCs, was identified in seized powder in Belgium (EMCDDA, 2020).

The SCs generally show potent agonist activity with low *in vitro* binding affinity (K_i) in the nM range and thus they exert their effects at the cannabinoid receptors CB1 and CB2 (Mogler et al., 2018; Musa et al., 2020). 5F-MDMB-PICA and 4F-MDMB-BICA were reported to be full agonists at the CB1 receptor showing higher efficacy than the full agonist JWH-018. However, in the literature, varied half-effective concentrations (EC_{50}) can be found in the range of 0.45–27.6 nM for 5F-MDMB-PICA obtained by variant binding assays (Cannaert et al., 2020; Musa et al., 2020; Truver et al., 2020; Janssens et al., 2022). Interestingly, changing the 5-fluoropentyl tail of 5F-MDMB-PICA to 4-fluorobutyl chain resulted in reduced efficiency for 4F-MDMB-BICA with an EC_{50} value of 121 nM in the CB1R β-arrestin 2 recruitment assay. A similar trend was observed for imidazole analogs 5F-MDMB-PINACA (EC_{50}: 0.84–1.78 nM) and 4F-MDMB-BINACA (EC_{50}: 5.69–7.39 nM) (Cannaert et al., 2020; Lie et al., 2021).

Nowadays, the hyphenated techniques, especially the targeted liquid chromatographic separation coupled to tandem mass spectrometry (LC-MS/MS) methods, are spread in the screening SCs (Krishnamurthy and Kadu, 2023). In forensic practice, detecting only the parent compounds of SCs, in particular, hours after consumption, cannot provide reliable information about their potential use because of their relatively short half-life (Institóris et al., 2022a). The rapid metabolism of SCs makes the analysis of their main characteristic metabolites necessary in order to obtain an accurate picture of drug abuse. However, critical questions arise about the drug influence on skills when only metabolites of a given SC are detectable and the concentration of the parent compound is lower than the limit of detection in the biofluids. The knowledge of quantitative data of main urinary metabolites and their potency and efficiency on CB1 receptor might be the first steps on this road. The term "polydrug use" refers to the consumption of two or more illicit drugs in combination in order to achieve greater and longer enjoyment value than that obtained by the use of a single component (Iudici et al., 2015). The spread of polydrug use, in addition to its recreational benefits, entails a number of still unclear health risks and forensic aspects, especially for drug influence (Wagner et al., 2014; Besli et al., 2015; Hutton, 2022; Janssens et al., 2022).

To the best of our knowledge, this is the first attempt to report quantitative results of the main urinary metabolites of 5F-MDMB-PICA and 4F-MDMB-BICA together, and their CB1 receptor binding affinities. Additionally, our experiments included the determination of urinary levels of other illicit drugs in order to investigate polydrug use. Regarding the pharmacological characterization of investigated SCs and their butanoic acid metabolites, this is the first study that describes the *in vitro* binding and signaling properties of 5F-MDMB-PICA, 4F-MDMB-BICA, and their major metabolites and compares their binding and signaling properties to those of THC and JWH-018 in brain membrane homogenates of the rat.

2. Materials and methods

2.1. Chemicals and standards

The 2-([1-(4-fluorobutyl)-1H-indole-3-carbonyl]amino)-3,3-dimethylbutanoate (4F-MDMB-BICA), (*S*)-2-(1-(4-fluorobutyl)-1H-indole-3-carboxamido)-3,3-dimethylbutanoic acid (4F-MDMB-BICA-COOH) and (*S*)-N-(1-amino-3-methyl-1-oxobutan-2-yl)-1-(4-fluorobenzyl)-1H-indazole-4,5,6,7-d4–3-carboxamide (AB-FUBINACA-d_4) as an internal standard were obtained from Cayman Chemicals (Ann Arbor, MI, USA). The 5F-MDMB-PICA (methyl-2-{[1-(5-fluoropentyl)indole-3-carbonyl]amino]}-3,3-dimethylbutanoate), (*S*)-2-(1-(5-fluoropentyl)-1H-indole-3-carboxamido)-3,3-dimethylbutanoic acid (5F-MDMB-PICA-COOH), and Δ^9-tetrahyrocannabinol (THC, 1 mg/mL EtOH) were provided by the Hungarian Institute for Forensic Sciences, Drug Laboratory (Szeged, Hungary). For all standards, the purity was higher than 98%. The standard solutions, prepared in ethanol, were stored at −20 °C. For urinary enzymatic hydrolysis, β-glucuronidase from *Helix pomatia* was used (Sigma Aldrich, St. Louis. MO, USA). All chemicals (LC-MS grade water (H_2O), methanol (MeOH), acetonitrile (ACN), ethyl acetate (EtOAc), 2-propanol (IPA), formic acid (FA), and HPLC-grade ammonia solution) for sample preparation and analytical measurement were from VWR (Radnor, PA, USA).

Buffer components (Tris, EGTA, $MgCl_2$), GDP, GTPgS were purchased from Sigma-Aldrich (Sigma Aldrich, St. Louis, MO, USA), fatty acid-free bovine serum albumin (BSA) was from VWR Life Science (Radnor, PA, USA). Rimonabant was obtained from Sigma-Aldrich (Sigma Aldrich, St. Louis. MO, USA), WIN-55,212–2 was purchased from Tocris Inc. (Bristol, UK). JWH-018 was prepared in the Laboratory of Chemical Biology (BRC, Hungary). [^{35}S]GTPgS (s.a. >37 TBq/mmol) was purchased from PerkinElmer (Waltham, MA, USA).

The radioligand [^{3}H]WIN-55,212–2 (specific activity 485 GBq/mmol) was prepared in the Laboratory of Chemical Biology (BRC, Hungary) (Dvorácskó et al., 2019). Tritium labeling was carried out in a self-designed vacuum manifold, and radioactivity was measured with a Packard Tri-Carb 2100 TR liquid scintillation analyzer using Insta Gel scintillation cocktail of PerkinElmer (Waltham, MA, USA). Drugs were dissolved at 1 mM in dimethyl sulfoxide (DMSO), stored at −20 °C, and then diluted in the binding buffer.

2.2. Sample preparation procedure of urine

The 22 urine samples were collected from police detainees suspected of drug abuse in sterile plastic urine containers and stored at +4 °C degrees till analysis. The selected samples were positive for 5F-MDMB-PICA and/or 4F-MDMB-BICA or their main metabolites during SC screening. The positive and control urine samples were stored at −80 °C until they were remeasured in one batch. The drug-free control urine samples were provided by volunteers. The study was performed with the approval of the Hungarian ethics committee (ETT TUKEB: BMEÜ/2326–1/2022/EKU) and with the local Ethical Committee of the University of Szeged (198/2022-SZTE –IKEB).

The sample preparation was as previously detailed (Körmöczi et al., 2022). Briefly, after the enzymatic hydrolysis of glucuronidated phase II metabolites of 5F-MDMB-PICA and 4F-MDMB-BICA, the reaction mixture was alkalized by ammonia solution (5 *v*/v%). The liquid-liquid extraction was applied with EtOAc. After the centrifugation, the upper phase was collected, evaporated, and the residual was dissolved in 200 μL 1:1:0.1 H_2O/ACN/FA (*v*/v/v%) mixture.

For quantitative analysis of urine samples, external calibration using internal standard was prepared with the following concentrations: 0, 0.05, 0.1, 0.2, 0.5, 1, 2, 5, 10, 25, 50, and 100 ng/mL for 5F-MDMB-PICA, 4F-MDMB-BICA parent compounds, 5F-MDMB-PICA-COOH, and 4F-MDMB-BICA-COOH main metabolites.

2.3. Targeted UHPLC-MS/MS parameters

The targeted analytical method was performed on Shimadzu Nexera (Kyoto, Japan) ultra-high-performance liquid chromatography (UHPLC) system coupled to TSQ Fortis triple quadrupole mass spectrometer (MS, Thermo Scientific, Waltham, MA, USA).

Chromatographic separations were performed using Kinetex C18 column (100 × 2.1 mm, 2.6 μm particle, with 4 × 2 mm, 5 μm guard column, Phenomenex, Torrance, CA, USA). The column was heated at 50 °C. The *A* eluent was 0.1% FA in H_2O, and 0.1% FA in ACN was used

for the *B* eluent. The applied low pressure gradient program was the following: 0 min - 40% B, 5 min - 80% B, 6 min - 100% B, 7.4 min - 100% B, 7.5 min - 40% B, 10 min - 40% B. The flow rate was kept at 0.4 mL/min till 6.5 min, then 0.9 mL/min in the range of 6.6–9.4 min, and the initial flow rate was set back at 0.4 mL/min at 9.5 min. The injector needle was washed with IPA/MeOH/H_2O/FA (70:25:5:0.1, *v*/v/v/v%) solution after each injection. The injection volume was 15 μL.

The tandem mass spectrometer was operated in positive electrospray ionization (ESI) mode. The capillary temperature was 300 °C, the vaporizer temperature was 350 °C, the spray voltage was 4.5 kV, the sheath gas flow was 50, the sweep gas flow was 1, and the auxiliary gas flow was 5 in arbitrary units. The positive ions were detected in selected reaction monitoring mode with FWHM at 0.7 resolution for both Q1 and Q3 quadrupole. The collision-induced dissociation gas was maintained at 1.5 mTorr. The flow injection method was used to determine the appropriate quantifier and qualifier ions of given protonated precursor ions and optimization of tandem mass spectrometric parameters (Fig. 1). The tube lens voltages were the followings: 5F-MDMB-PICA (107 V), 4F-MDMB-BICA (117 V), 5F-MDMB-PICA-COOH (114 V), and 4F-MDMB-BICA-COOH (120 V).

The LabSolution Verison 5.97 SP1 (Shimadzu, Kyoto, Japan) software was used for controlling the UHPLC system. For data acquisition, postprocessing and quantitative evaluation of MS/MS raw file Xcalibur 4.2 software was used (Thermo Fisher Scientific, Waltham, MA, USA). The unpaired *t*-test was performed by GraphPad Prism 5.0 (GraphPad Software, San Diego, CA, USA).

2.4. Validation of UHPLC-MS/MS method for the analysis of SCs

The UHPLC-MS/MS method was validated for the analysis of 5F-MDMB-PICA, 5F-MDMB-PICA-COOH, and 4F-MDMB-BICA-COOH in human urine samples. The validation process is detailed in the Supplementary Information. For 4F-MDMB-BICA, the validation of the targeted method was already published (Körmöczi et al., 2022.)

2.5. Preparation of brain membrane homogenates

The preparation of rat brain tissue membrane homogenates was performed according to our previously published articles (Dvorácskó et al., 2019; Stefanucci et al., 2018; Dimmito et al., 2019).

Briefly, male Wistar rats were locally bred and handled following the EU Directive 2010/63/EU and the Regulations on Animal Protection (40/2013. (II. 14.) Korm. r.) of Hungary. Male rats were anaesthetized with CO_2, and brains were quickly removed and put in ice-cold 50 mM Tris–HCl buffer (pH 7.4), then homogenized with a Braun Teflon-glass homogenizer at the maximum rpm. In the next step, the homogenate was centrifuged at 20,000 g for 25 min, after the suspended pellet was incubated at 37 °C for 30 min. The centrifugation step was repeated. The final pellets were suspended and homogenized with a glass potter in five volumes of 50 mM Tris-HCl (pH 7.4) buffer that contains 0.32 M sucrose and stored at −80 °C. The protein concentration was determined by the Bradford method. These membrane homogenates were used either in radioligand displacement assay or in [^{35}S]GTPγS functional assays.

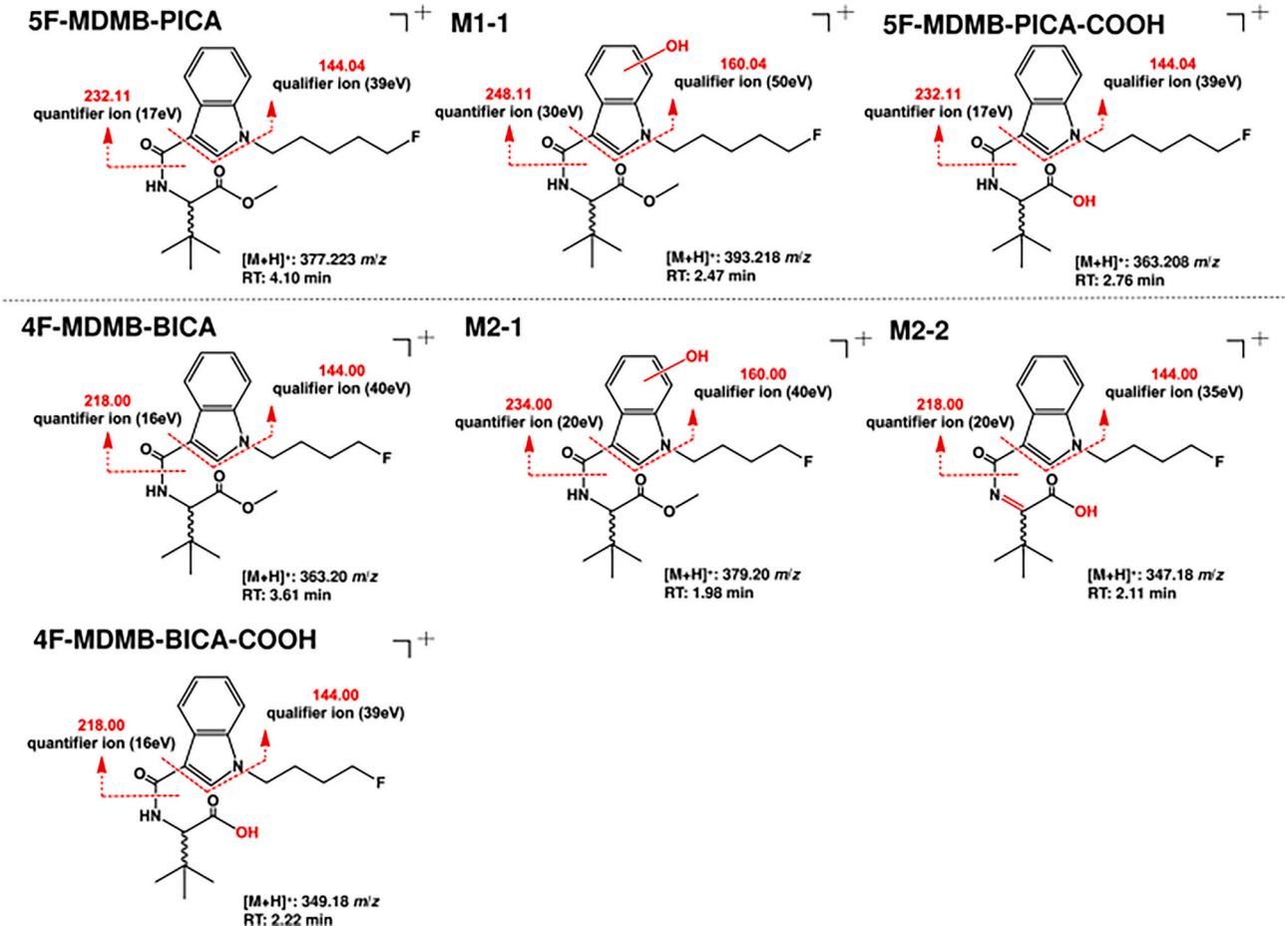

Fig. 1. Structure of 5F-MDMB-PICA and 5F-MDMB-PICA mono-hydroxylated metabolite (M1–1), 5F-MDMB-PICA-COOH, 4F-MDMB-BICA and 4F-MDMB-BICA mono-hydroxylated metabolite (M2–1), 4F-MDMB-BICA ester hydrolysis + dehydrogenation phase I product (M2–2), and 4F-MDMB-BICA-COOH with observed *m/z* values, their proposed related fragmentations (with collision energy) and retention times.

2.6. Radioligand competition binding assay

Binding assays using [^{3}H]WIN55,212–2 were performed as reported previously (Dvorácskó et al., 2019; Stefanucci et al., 2018; Dimmito et al., 2019).

Briefly, 0.5 mg/mL rat membrane homogenates were resuspended in 1 mL of binding buffer (50 mM Tris-HCl binding buffer (pH 7.4), 2.5 mM EGTA, 5 mM $MgCl_2$, and 0.5 mg/mL fatty acid-free BSA) in plastic tubes and co-incubated with different concentrations (10^{-11}–10^{-5} M) of various unlabeled ligands and 6 nM of [^{3}H]WIN55,212–2 (K_d: 10.1 nM) for 60 min at 30 °C. Nonspecific binding was determined in the presence of 10 μM WIN 55212–2. The incubation was stopped by diluting the samples with ice-cold wash buffer (50 mM Tris-HCl, 2.5 mM EGTA, 5 mM $MgCl_2$, 0.5% fatty acid-free BSA, pH 7.4), followed by repeated washing and rapidly filtered through a 0.1% polyethyleneimine pre-soaked Whatman GF/B glass fiber filters. For filtration, the 24-well Brandel Cell Harvester was used, and the filters were immersed into Ultima Gold MV scintillation liquid. The radioactivity measurements were performed by TRI-CARB 2100TR counter (Packard, PerkinElmer, Waltham, MA, USA).

2.7. Ligand stimulated [^{35}S]GTPγS binding assay

Agonist stimulated [^{35}S]GTPγS binding assays were carried out as described previously (Dvorácskó et al., 2019; Stefanucci et al., 2018; Dimmito et al., 2019).

Briefly, 30 μg brain membrane homogenate per tube was diluted in assay buffer (50 mM Tris-HCl buffer (pH 7.4), 100 mM NaCl, 3 mM $MgCl_2$, 1 mM EGTA and 30 μM GDP) incubated with 0.05 nM [^{35}S]GTPγS (PerkinElmer) and different concentrations (10^{-11}–10^{-5} M) of various unlabeled ligands for 60 min at 30 °C. Nonspecific binding was determined in the presence of 10 μM unlabeled GTPγS. Incubation, filtration, and radioactivity measurements steps are the same as described in 2.6. part.

2.8. Data analysis of in vitro biological assays and in vitro radioligand binding assay

Results are expressed as means ± SEM of at least three independent experiments, each performed in duplicate or triplicate. The competition binding data evalution were detailed in our previous paper (Dvorácskó et al., 2021).

In [^{35}S]GTPγS binding studies, data were expressed as the percentage stimulation of the specific [^{35}S]GTPγS binding over the basal activity and are given as means ± SEM. Each experiment was analyzed with a sigmoid dose-response curve fitting to obtain potency (EC_{50}) and efficacy (E_{max}) values. One-way ANOVA followed by the Bonferroni's multiple comparison test was used to statistically compared E_{max} and EC_{50} values (***, $P < 0.001$; **, $P < 0.01$; *, $P < 0.1$, GraphPad Prism 5.0, San Diego, CA, USA).

3. Results

3.1. Validation of targeted UHPLC-MS/MS method for analysis of SCs

In our previous paper, we were the first to report 20 urinary and 13 blood *in vivo* phase I metabolites of 4F-MDMB-BICA, and the ester hydrolysis metabolic product was suggested as the primary biomarker in both urine and blood. For urine samples, the mono-hydroxylation metabolite while the ester hydrolysis + dehydrogenation phase I product were selected in blood as secondary confirmatory targets for the screening of 4F-MDMB-BICA (Körmöczi et al., 2022).

For UHPLC-MS/MS analysis of 5F-MDMB-PICA, 4F-MDMB-BICA, 5F-MDMB-PICA-COOH, and 4F-MDMB-BICA-COOH, the mass spectrometric parameters of the selected transitions (quantifier and qualifier ions) were optimized, and the targeted method was updated. The analytical method was validated for urinary quantification of investigated SCs with the recovery, matrix effect, process efficiency, limit of detection (LOD), limit of quantification (LOQ), linearity, accuracy, precision, carry-over, and stability. The validation method, criteria, and obtained validation results for targeted compounds are summarized in Supplementary Information and **Table S1**. The methanol solution of standard SCs was infused at 5 μL/min through static mixing tee in the initial UHPLC eluent flow at 395 μl/min of flow rate and then introduced into the ESI source. For targeted UHPLC-MS/MS analysis, two transitions per compound were selected for quantitative analysis and qualitative confirmation with a related retention time window. The proposed fragmentation pathways of SCs with optimized collision voltage are shown in Fig. 1. The obtained validation results are summarized in linear regression analysis was used to determine the limit of linearity of the assay, and the concentration range was found from 0.2 to 25 ng/mL, with the coefficient of determination (R^2) being greater than 0.980 for all components. For 5F-MDMB-PICA and its ester hydrolyzed metabolite, the targeted UHPLC-MS/MS method provided 0.005 ng/mL and 0.005 ng/mL of LOD, while 0.030 ng/mL was obtained for 4F-MDMB-BICA metabolite. Concerning LOQ values, 0.015 ng/mL for 5F-MDMB-PICA, 0.014 ng/mL for 5F-MDMB-PICA-COOH, and 0.090 ng/mL for 4F-MDMB-BICA ester hydrolyzed metabolite were determined. For 5F-MDMB-PICA and 5F-MDMB-PICA-COOH, the obtained LOD and LOQ values were better than those in the literature published previously (Kleis et al., 2020; Krotulski et al., 2021; Tokarczyk et al., 2022; Szpot et al., 2022; Wu et al., 2023). The accuracy was passed within the accepted bias of ±30% in three concentration levels. Within-run and between-run precision data for all compounds were within the acceptable limits ranging in coefficient of variation (%CV) from 0.00 to 8.7%. The process efficiency values were in the range of 63.3–97%. Studying recovery and matrix effect helps to understand their contribution to obtained process efficiency. Recovery for all compounds was between 53% and 88%. ESI leads to a slight ion enhancement effect up to 34% of the matrix effect value for all compounds in three concentration levels. During the validation of an analytical method, an important aspect is the examination of the stability of the investigated compounds. The processed samples of urine extracts have satisfactory stability for all analytes. No significant analyte loss was noted in any of the QC, suggesting that samples awaiting analysis are stable for up to 3 days both in urine and in the extract form. The calculated carry-over of compounds was also negligible (< 0.01%). Overall, the obtained main validation parameters verify that our targeted UHPLC-MS/MS method with related sample preparation procedures is suitable to screen both 5F-MDMB-PICA and 5F-MDMB-PICA ester hydrolyzed metabolites as well as 4F-MDMB-BICA and 4F-MDMB-BICA ester hydrolyzed metabolites in human urine samples.

3.2. Screening of 5F-MDMB-PICA, 4F-MDMB-BICA, 5F-MDMB-PICA-COOH, and 4F-MDMB-BICA-COOH

In the screening of urine samples for 5F-MDMB-PICA-COOH and 4F-MDMB-BICA-COOH metabolites were analyzed beside the parent molecules. In order to quantify the main metabolites of 5F-MDMB-PICA and 4F-MDMB-BICA, the ester hydrolysis metabolic products were selected as primary biomarker targets (5F-MDMB-PICA-COOH for 5F-MDMB-PICA and 4F-MDMB-BICA-COOH for 4F-MDMB-BICA) according to Giorgetti's suggestions and our previous study (Giorgetti et al., 2022; Körmöczi et al., 2022). As the selection of primary confirmatory targets, the mono-hydroxylation products (M1–1 and M2–1) of both parent compounds and ester hydrolysis + dehydrogenation metabolites (M2–2) of 4F-MDMB-BICA were added as additional target ion to the analytical method (Qin et al., 2022; Körmöczi et al., 2022). The appropriate transitions with related main chromatographic and optimized tandem mass spectrometric parameters of seven investigated analytes are summarized in Fig. 1. For quantitative and semi-quantitative comparisons of targeted compounds, 22 positive drug urine samples were analyzed in

one batch. The concentration values were given only for compounds with standards available. The obtained quantitative and qualitative data are summarized in **Table S**2. In the case, when the level of the parent molecule is lower than LOD, the urine sample is positive for SC if both metabolites can be detected. Abuse of 5F-MDMB-PICA could be determined in 12 of the 22 urine samples examined, while 11 were positive for 4F-MDMB-BICA. By comparing the median concentration values of parent compounds of two SCs, in the case of 4F-MDMB-BICA, higher urinary levels (0.312 ng/mL) were obtained than for 5F-MDMB-PICA (0.076 ng/mL). In the literature, few quantitative data have been found for the urinary concentration of 5F-MDMB-PICA and 4F-MDMB-BICA, and only qualitative information is available for their metabolites (Kleis et al., 2021; Tokarczky et al. 2022; Institóris et al., 2022b). Naturally, in the absence of information of the exact time of consumption and the amount of SCs administered, including other not controlled parameters, no conclusions can be drawn from the obtained values. However, it is clear that the analysis of the main metabolites has great importance in forensic practice. This is well demonstrated by the fact that the parent compound of 4F-MDMB-BICA was detected in only 3 cases and 5F-MDMB-PICA molecular ion in 9 samples of 22 samples.

For the urinary levels of a butanoic metabolite of 5F-MDMB-PICA, the concentration range was 0.029–881.02* ng/mL, and the concentration of 4F-MDMB-BICA-COOH was found to be 0.396–4579* ng/mL. The obtained high metabolite concentrations support their fast metabolism theory by examining the main metabolite/parent molecule urinary level ratio (Institóris et al., 2022a).

3.3. Urinary level of 5F-MDMB-PICA and 4F-MDMB-BICA in polydrug use aspect

In this study, the urinary samples investigated were also screened for classic narcotics, stimulants, opiates, and benzodiazepines, as detailed in **Table S2**. The obtained concentration results are summarized in **Table S1**. The routine forensic GC-MS analysis of 22 urine samples confirmed the abuse of the following illicit drugs besides 5F-MDMB-PICA and 4F-MDMB-BICA: THC, *N*-ethylhexedrone, 3,4-methylenedioxymethamphetamine (MDMA), 3,4-Methylenedioxyamphetamine (MDA), chlonazepam, amphetamine, and alprazolam in 19 cases. The results clearly show that *N*-ethylhexedrone and THC were used most often in combination with SCs in 68% of 22 suspects. The concentration range of *N*-ethylhexedrone was 173–14,087 ng/mL, which was in good agreement with the concentration found with suspected drug-influenced drivers reported by Institóris *et al.* (Institóris et al., 2022b). MDMA and MDA are also frequently used in combination with other illicit drugs. For these three urine samples, MDMA and MDA were detected besides 5F-MDMB-PICA (1) and 4F-MDMB-BICA (2). For comparing these samples, the presence of THC-COOH and *N*-etylhexedrone was additionally confirmed for only the 4F-MDMB-BICA positive samples. For the number 13 sample, the use of the highest number of illicit drugs was verified, including 4F-MDMB-BICA, THC, *N*-ethylhexedrone, MDMA, MDA, chlonazepam, and alprazolam. In Fig. 2, the calculated mean and median concentrations of seven illicit drugs and metabolites are summarized and detailed according to their combination with 5F-MDMB-PICA or 4F-MDMB-BICA, or both of them. Comparable concentration results were observed for the seven compounds in both 5F-MDMB-PICA and 4F-MDMB-BICA positive samples. For samples containing both *N*-ethylhexedrone and 4F-MDMB-BICA, higher mean and median concentration

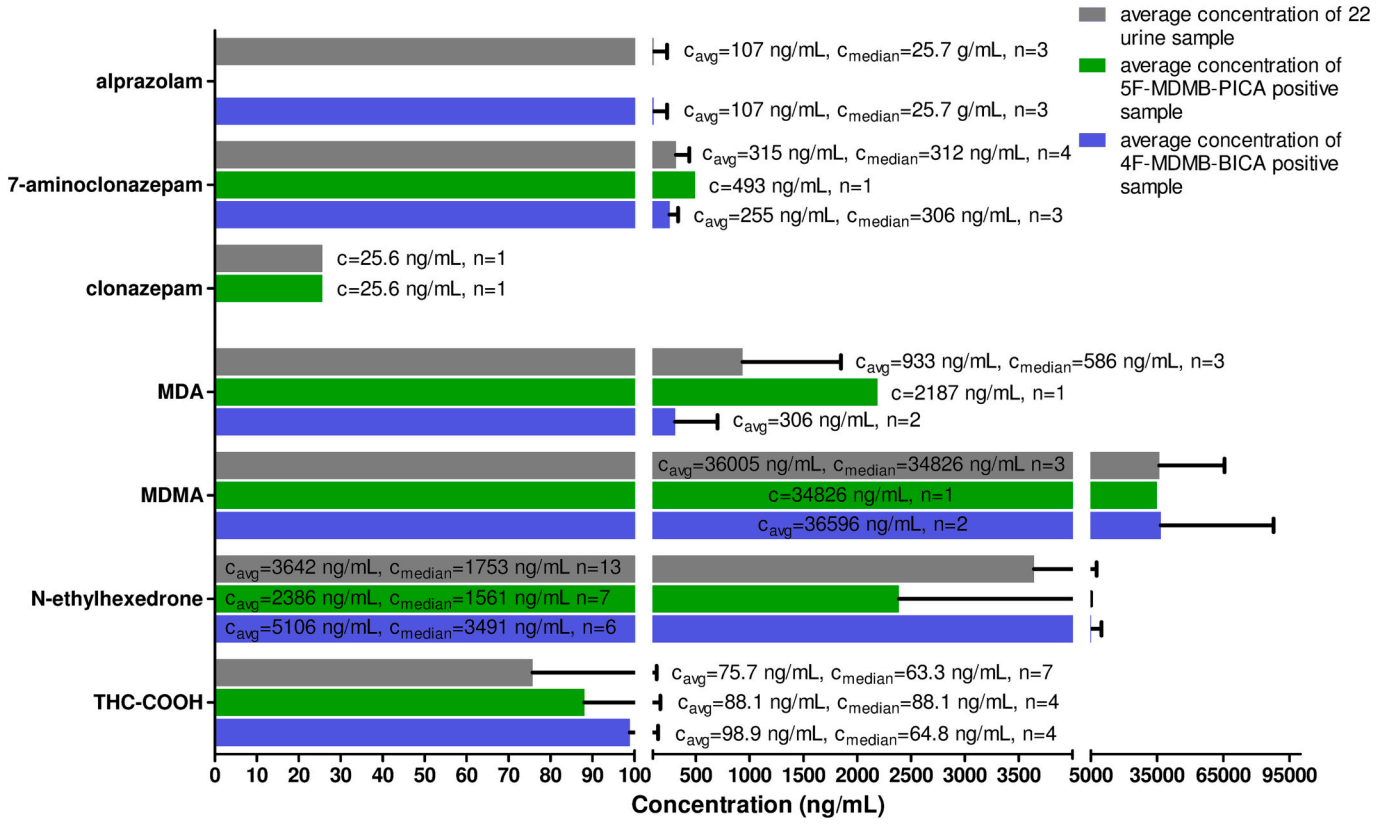

Fig. 2. The calculated mean concentration (c_{avg}) of sevenillicit drugs and metabolites (THC-COOH, *N*-ethylhexedrone, MDMA, MDA, clonazepam, 7-aminoclonazepam, alprazolam) in 22 urine samples (gray columns), the mean concentration of seven illicit drugs in 5F-MDMB-PICA positive samples (green columns), and the mean concentration of seven illicit drugs in 4F-MDMB-BICA positive samples (blue columns) with calculated median concentration (c_{median}) and the number of samples (n). The standard deviations are labeled on the columns. (For interpretation of the references to colour in this figure legend, the reader is referred to the web version of this article.)

values were obtained than in samples with a combination of 5F-MDMB-PICA and *N*-ethylhexedrone. However, this difference was not statistically significant.

The combination of SCs is also frequent among consumers. Interestingly, only number 12 of the urine samples was positive for both SCs. Fig. 3 represents the extracted ion chromatogram of the number 15 urine sample, which was positive for 4F-MDMB-BICA, because of detected M2–1, M2–2, and 4F-MDMB-BICA-COOH metabolites as well as the parent compound. However, only the 5F-MDMB-PICA-COOH metabolite was detectable; therefore, the urine sample was designated as negative for 5F-MDMB-PICA.

3.4. Pharmacological characterization of 5F-MDMB-PICA, 4F-MDMB-BICA, and their main urinary metabolites

Two novel SCs, 5F-MDMB-PICA and 4F-MDMB-BICA which differ only in a single methylene group at the tail, and the carboxylic acid metabolites of these methyl esters were studied for their binding properties to cannabinoid receptor 1 (CB1R) and for their ability to activate G protein-coupled receptors in rat brain membrane homogenate that abundantly contains CB1 receptors (Sim et al., 1995; Dvorácskó et al., 2019; Zádor et al., 2020; Mollica et al., 2017).

The CB1R binding affinities of the SCs were determined in competitive binding assays using the radioligand [^{3}H]WIN55,212–2. The assay conditions were validated with the reference cannabinoid compounds THC and JWH-018. It was found that both 5F-MDMB-PICA and 4F-MDMB-BICA exhibited nanomolar affinity to the [^{3}H]WIN55,212–2 binding sites, and both SCs displaced almost 100% of the radioligand. 5F-MDMB-PICA had the highest binding affinity to the CB1R (K_i = 0.38 nM), which was 121-fold and 8-fold higher than that of THC and JWH-018, respectively. In our system, the constant inhibitory value of 5F-MDMB-PICA against [^{3}H]WIN55,212–2 was 14-times higher than that reported by Janowsky (K_i = 5.4 nM) on HEK cells using the radioligand [^{3}H]CP-55,940 (WHO, 2019). The differences between our binding results and those reported by Janowsky *et al.* could be attributed to the use of different membrane homogenates (HEK cells vs rat brain) and different radioisotopes.

In the case of 4F-MDMB-BICA, where the indole *N*-substituent 5-fluoro-1-alkyl chain is shorter, the CB1R binding affinity was found to be 16-fold weaker, but still nanomolar (K_i = 6.4 nM), than that of the homologue SC 5F-MDMB-PICA as compared to THC and JWH-018. The 4F-MDMB-BICA exhibited 7-fold higher and twice lower CB1R binding affinity. Currently, no information is available about the *in vitro* displacement studies of 4F-MDMB-BICA. The constant inhibitory values of 4F-MDMB-BINACA and the indazole homologue of 4F-MDMB-BICA was reported to be 14.3 nM on HEK cells in the presence of the radioligand [^{3}H]CP-55,940 (WHO, 2019).

The affinity of the main butanoic acid metabolites to the [^{3}H]WIN55,212–2 labelled binding sites significantly decreased as compared to the methyl ester SCs. 5F-MDMB-PICA-COOH was able to compete with [^{3}H]WIN55,212–2, with an apparently high inhibitory constant of 3.2 μM, whereas 4F-MDMB-BICA-COOH displaced only 80% of the radioligand with a constant inhibitory value of 2.9 μM. The obtained concentration range of inhibitory constant for 5F-MDMB-PICA-COOH agrees with the value of its indazole analog 5F-MDMB-PINACA-COOH (1.9 μM) newly reported by Cabanlong *et al.* (Cabanlong et al., 2022). In our experimental model, the investigated compounds competed for the [^{3}H]WIN55,212–2 labeled binding sites with the following order of binding affinities: 5F-MDMB-PICA > JWH-018 > 4F-MDMB-BICA > THC > > 4F-MDMB-BICA-COOH >5F-MDMB-PICA-COOH (Fig. 4A, Table 1). A similar trend was reported in the rank of affinity for 5F-MDMB-PINACA, its butanoic acid metabolite, and THC using radioligand [^{3}H]CP-55,940 in mouse brain homogenates (Cabanlong et al., 2022).

In order to determine whether the SC parent ligands and their metabolites are able to stimulate the CB1R-associated G proteins (GPCR), these compounds were subjected to ligand-stimulated [^{35}S]GTPγS binding assays in rat brain membrane homogenate. This assay directly measures the early event after GPCR activation. It was found that 5F-MDMB-PICA and 4F-MDMB-BICA were 31-times and 7.4-times more efficacious, respectively, than the partial agonist THC and they acted as full agonists. 5F-MDMB-PICA increased the G-protein basal activity up to a maximum efficacy of 191% and with a high potency of 7.8 nM (Fig. 4B, Table 1). The stimulatory activity of the butyl homolog 4F-MDMB-BICA was slightly lower (E_{max} = 179%), and its potency was 4-fold lower than that of 5F-MDMB-PICA. The efficacy of 5F-MDMB-PICA and 4F-MDMB-BICA was 37% and 25% greater, respectively, than that of the prototypical synthetic cannabinoid JWH-018. 5F-

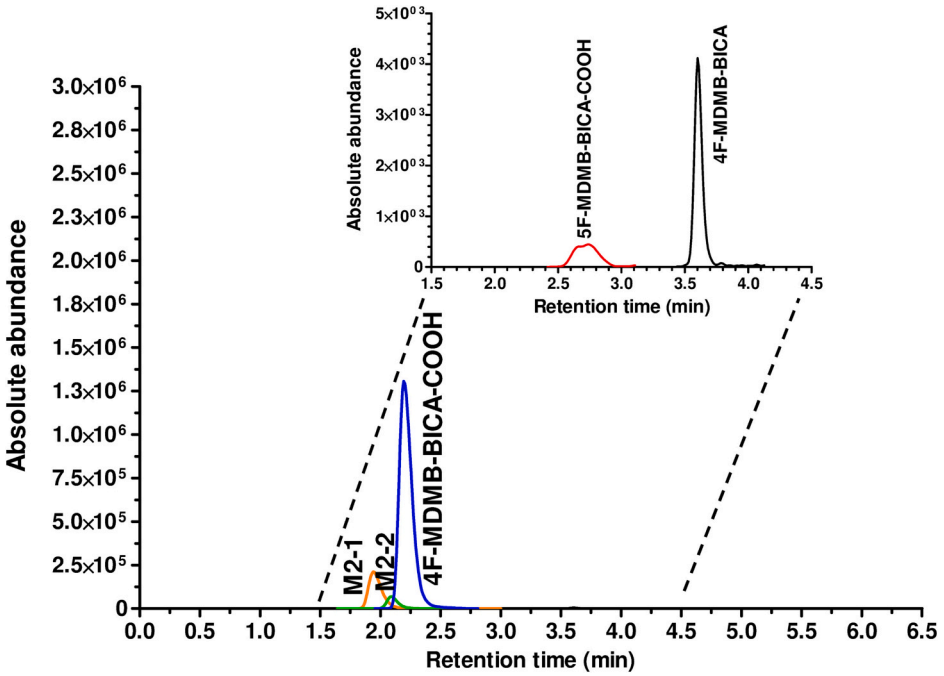

Fig. 3. UHPLC-MS/MS extracted ion chromatogram of number 15 urine sample.

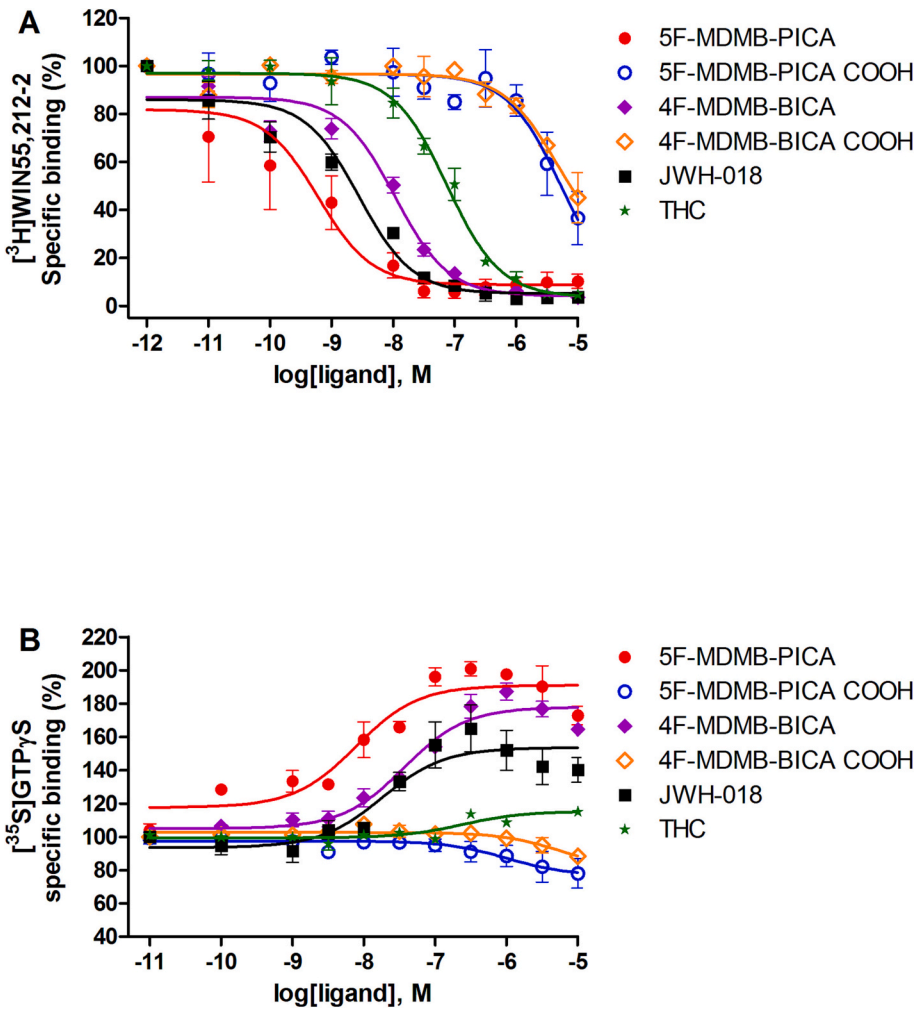

Fig. 4. (A) Cannabinoid receptor binding affinity of THC, JWH-018, novel synthtetic cannabinoids, and their butanoic acid metabolites in [3H]WIN55,212–2 competition binding assays to rat whole brain membrane homogenates. Figures represent the specific binding of the radioligand in percentage in the presence of increasing concentrations (10^{-11}–10^{-5} M) of the indicated ligands. Data are expressed as a percentage of mean specific binding ± SEM. ($n \geq 3$). The affinity values (K_i) of the unlabeled compounds are indicated in Table 1. (B) G protein activation effects of the indicated ligands in [^{35}S]GTPγS binding assays in rat brain membrane homogenates. Figures represent relative specific binding of [^{35}S]GTPγS in the presence of increasing concentrations (10^{-10}–10^{-5} M) of the indicated compounds. Data are expressed as a percentage of mean specific binding ± SEM. ($n \geq 3$). The maximum efficacy (Emax) and potency (EC_{50}) values of the unlabeled compounds are indicated in Table 1.

Table 1
In vitro binding affinity (K_i) and signaling efficacy (E_{max}) and potency (EC_{50}) of synthetic cannabinoids and and their carboxylic acid metabolites.

compounds	K_i ± SEM [^{3}H]WIN55,212–2 binding (nM)	[^{35}S]GTPγS binding	
		E_{max} ± SEM (%)	EC_{50} ± SEM (nM)
JWH-018	3.2 ± 0.6	154 ± 3.9	18 ± 2.5
THC	46 ± 5.1	116 ± 3.7	245 ± 21
5F-MDMB-PICA	0.38 ± 0.02	191 ± 4.1	7.8 ± 2.1
5F-MDMB-PICA COOH	3216 ± 414	77 ± 5.2	1016 ± 19
4F-MDMB-BICA	6.4 ± 0.6	179 ± 2.8	33 ± 3.1
4F-MDMB-BICA COOH	2881 ± 216	80 ± 9.3	2892 ± 357

K_i values were calculated from the corresponding displacement curves of Fig. 2. (**A**). The E_{max} and EC_{50} values were calculated from the dose-response curves of Fig. 2. (**B**). Each data represents the mean ± SEM from least 3 independent experiments.

MDMB-PICA was 2.3-times more potent than JWH-018, while 4F-MDMB-BICA was 1.8-times less potent than JWH-018. In our system, truncation of the alkyl chain of 5F-MDMB-PICA resulted in a decrease in both efficacy and potency, in harmony with the agreement of Cannaert *et al.* in the *in vitro* β-arrestin 2 recruitment assay. In contrast, no dramatic reduction can be observed in the G-protein activation of 4F-MDMB-BICA, with only a 4-time decrease in potency and a drop of 12% in efficacy compared to that of 5F-MDMB-PICA (Cannaert et al., 2020). However, our EC_{50} results only partially agree with previous findings and the E_{max} values were lower than those reported previously in the β-arrestin-based assay. Finally, the 5F-MDMB-PICA > JWH-018 > 4F-MDMB-BICA relative rank order of potency was similar (Banister et al., 2016; Noble et al., 2019; Cannaert et al., 2020; Truver et al., 2020).

The hydrolysis of the methyl ester function of 5F-MDMB-PICA and 4F-MDMB-BICA results in carboxylic acid metabolites. It was found that the full agonist character of the methyl esters changed to a weak inverse agonist/antagonist after ester hydrolysis. The maximum efficacy of 5F-MDMB-PICA-COOH and 4F-MDMB-BICA-COOH was between 77% and 80%, and their potency was between 1 μM and 2.8 μM (Fig. 4B, Table 1). The introduction of the carboxyl functional group in 5F-MDMB-PICA and 4F-MDMB-BICA gave a weak inverse agonist. This is in agreement with our previous work with ADB-FUBINACA/rimonabant hybrids (Stefanucci et al., 2018). Interestingly, for 5F-MDMB-PINACA-COOH, Cabanlong et al. reported the potency (EC_{50}: 5,5 μM) was five times lower but was in the same micromolar range that we found in our physiological system for 5F-MDMB-PINACA-COOH (EC_{50}: 1,1 μM). However, the 5F-MDMB-PINACA-COOH was found to remain an agonist similar to its parent compound, while our results suggested a 5F-MDMB-PICA-COOH ligand switched to a weak inverse agonist. (Cabanlong et al., 2022).

To explore the CB1R-mediated inverse agonist/antagonist effects of 5F-MDMB-PICA and 4F-MDMB-BICA metabolites, the G-protein activation of 5F-MDMB-PICA and 4F-MDMB-BICA was investigated in the absence or presence of the corresponding carboxylic acid metabolites, or

the control CB1 inverse agonist rimonabant in rat brain membrane homogenate by [^{35}S]GTPγS binding assays. The G-protein stimulatory effect of the full agonist 5F-MDMB-PICA was reduced by 20% or 66% in the presence of 1 μM or 10 μM 5F-MDMB-PICA butanoic acid metabolite, respectively. In the case of the potent agonist 4F-MDMB-BICA, maximum efficacy decreased by 22% or 49% in the presence of 1 μM or 10 μM 4F-MDMB-BICA butanoic acid metabolite. In both cases, the CB1R inverse agonist rimonabant decreased the stimulatory effect of the two SC agonists under the basal level. These results strongly indicate the dose-dependent CB1R-mediated weak inverse agonist effects of the two butanoic acid metabolites. The strong inhibitory effect of rimonabant was in agreement with its full inverse agonist effect (Fig. 5, Table 2).

Table 2
Calculated parameters of the antagonist effect of 5F-MDMB-PICA and 4F-MDMB-BICA butanoic acid metabolites and rimonabant in agonist induced [^{35}S]GTPγS binding assays in rat brain membrane homogenates.

compounds	[^{35}S]GTPγS binding	
	E_{max} ± SEM (%)	EC_{50} ± SEM (nM)
5F-MDMB-PICA	191 ± 4.1	7.8 ± 2.1
+ 1 μM 5F-MDMB-PICA COOH	171 ± 5***	4.1 ± 2.9
+ 10 μM 5F-MDMB-PICA COOH	125 ± 7.1***	0.9 ± 0.1**
+ 1 μM rimonabant	88 ± 3.2***	n.r.
+ 10 μM rimonabant	43 ± 2.8***	n.r.
4F-MDMB-BICA	179 ± 2.8***	33 ± 3.1
+ 1 μM 4F-MDMB-BICA COOH	157 ± 4.7***	30 ± 2.4
+ 10 μM 4F-MDMB-BICA COOH	130 ± 5.6***	40 ± 5.1*
+ 1 μM rimonabant	82 ± 2.4***	n.r.
+ 10 μM rimonabant	55 ± 5.6***	n.r.

Calculated maximal G-protein stimulation efficacy (E_{max}) and ligand potency (EC_{50}) values of the agonists 5F-MDMB-PICA and 4F-MDMB-BICA in the absence or presence of 1 μM or 10 μM of 5F-MDMB-PICA and 4F-MDMB-BICA butanoic acid metabolites or rimonabant. Statistical comparison of the E_{max} and EC_{50} values were performed by one-way ANOVA followed by the Bonferroni multiple comparison test (***, $P < 0.001$; **, $P < 0.01$; *, $P < 0.1$). n.r. not relevant.

4. Discussion

This is the first attempt to quantitatively analyze 5F-MDMB-PICA, 4F-MDMB-BICA, and their butanoic acid main metabolites in human urine samples in a quantitative manner using our validated targeted UHPLC-MS/MS method. For 5F-MDMB-PICA and 5F-MDMB-PICA-COOH, lower LOD and LOQ values were obtained than the literature data. Up to our knowledge, it is the first time to publish LOD and LOQ values of 4F-MDMB-BICA-COOH for biological samples. A primary question was how the 5F-MDMB-PICA-COOH and 4F-MDMB-BICA-COOH parent molecules in urine compare quantitatively with their primary metabolites. The urinary concentrations of the 5F-MDMB-PICA-COOH and 4F-MDMB-BICA-COOH metabolites spanned a more extensive range compared to the parent molecules. Specifically, the corresponding data found are 0.029–881.02* ng/mL for 5F-MDMB-PICA-COOH, 0.396–4579* ng/mL for 4F-MDMB-BICA-COOH, while 0.050–11.39 ng/mL for 5F-MDMB-PICA and 0.023–0.411 ng/mL for 4F-MDMB-BICA were found. Our study extended to investigate the combination of other illicit drugs with 5F-MDMB-PICA and 4F-MDMB-BICA. Eight illicit drugs and metabolites were analyzed by investigating the polydrug use of 22 urine samples, such as THC-COOH, *N*-ethylhexedrone, MDMA, MDA, clonazepam, 7-aminoclonazepam, amphetamine, and alprazolam in 19 cases. *N*-ethylhexedrone was to be combined most frequently with both SCs in the urinary concentration of 173–14,087 ng/mL range in 13 cases. Interestingly, the 5F-MDMB-PICA and 4F-MDMB-BICA combinative use was verified only in a single sample. Overall, the obtained results confirm the great importance of the targeted analysis of the main characteristic metabolites of SCs in the screening procedure. Another important question from a forensic point of view is the CB1 receptor binding properties of the parent compounds and their primary metabolites. We studied the binding properties of 5F-MDMB-PICA, 5F-MDMB-PICA-COOH, 4F-MDMB-BICA, and 4F-MDMB-BICA-COOH in one study first. According to our results, the following order of binding affinity was determined: 5F-MDMB-PICA > JWH-018 > 4F-MDMB-BICA > THC > > 4F-MDMB-BICA-COOH >5F-MDMB-PICA-COOH. Regarding the parent compounds, 5F-MDMB-PICA had binding affinities 121-fold and 8-fold higher than that of THC and JWH-018. Interestingly, the contribution of tail length for binding affinity was found to be determinative as the values of 4F-MDMB-BICA with a tail shorter by one methylene group has 16-fold lower than were for 5F-MDMB-PICA. However, the constant inhibitory values of butanoic acid metabolites were in the μM range compared with nM concentration of the parent compound. Consequently, 5F-MDMB-PICA-COOH and 4F-MDMB-BICA-COOH presumably might cause a lower psychoactive effect. The study of CB1R-mediated inverse agonist/antagonist effects of 5F-MDMB-PICA-COOH and 4F-MDMB-BICA-COOH revealed that the butanoic acid metabolites have dose-dependent CB1R-mediated weak inverse agonist effects.

According to our *in vitro* displacement and functional assays, the 5F-MDMB-PICA, 4F-MDMB-BICA primary metabolites retained affinity and efficacy at CB1R. Additionally, the high urinary concentration of the main metabolites highlighted that they might be relevant to the overall pharmacological profile following SCs consumption. The weaker but detected binding capacity of the metabolites when the parent compound is not present or in low concentration anymore may result in an elongated subjective experience of drug consumption or "post-drug symptoms", which may have clinical or even forensic consequences. However, further *in vivo* studies are necessary to clarify this issue.

Credit authorship contribution statement

Szabolcs Dvorácskó: methodology, data curation, writing - original draft. Tímea Körmöczi: methodology, data curation, writing - original draft. Éva Sija: methodology, data curation. Balázs Bende: ethics part, review. Review: Roland Weizner, Tibor Varga, István Ilisz, László

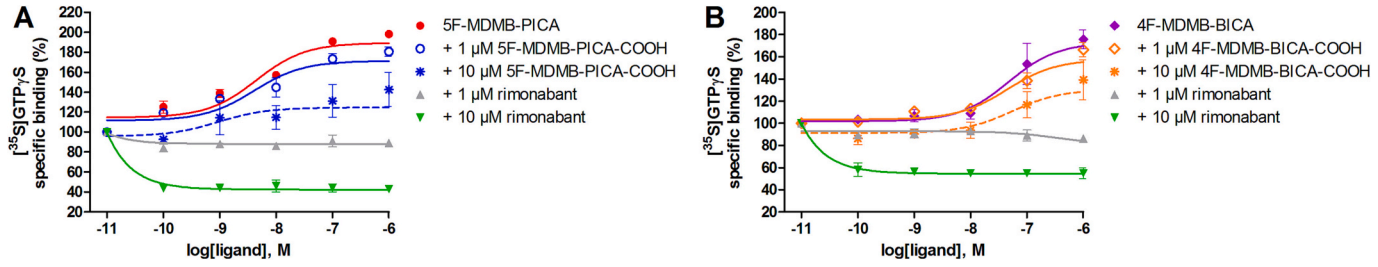

Fig. 5. The cannabinoid receptor-mediated antagonist effect of (A) 5F-MDMB-PICA and (B) 4F-MDMB-BICA butanoic acid metabolites in agonist-induced [^{35}S]GTPγS binding assays in rat brain membrane homogenates. Figures represent relative specific binding of [^{35}S]GTPγS with the increasing concentrations (10^{-10}–10^{-5} M) of 5F-MDMB-PICA and 4F-MDMB-BICA in the absence or in the presence of 1 μM or 10 μM of (A) 5F-MDMB-PICA and (B) 4F-MDMB-BICA butanoic acid metabolites or rimonabant. Data are a mean percentage of specific binding ± SEM (n ≥ 3) over the basal activity of 100%. The calculated parameters are listed in Table 2.

Institóris, Éva M. Kereszty, Csaba Tömböly. Róbert Berkecz: conceptualization, methodology, data curation, writing - original draft, review, and editing. All authors approved the manuscript and its submission to this journal.

Declaration of Competing Interest

The authors declare the following financial interests/personal relationships which may be considered as potential competing interests:

Robert Berkecz reports financial support and equipment, drugs, or supplies were provided by Ministry of Innovation and Technology of Hungary from the National Research. Robert Berkecz reports a relationship with National Research, Development, and Innovation Office-NKFIA that includes: funding grants.

Data availability

Data will be made available on request.

Acknowledgement

The EU-funded Hungarian grant EFOP-3.6.1-16-2016-00008 founded this research. Project no. TKP2021-EGA-32 has been implemented with the support provided by the Ministry of Innovation and Technology of Hungary from the National Research, Development and Innovation Fund, financed under the TKP2021-EGA funding scheme. This work was also supported by National Research, Development, and Innovation Office-NKFIA through projects: National Laboratory of Translational Neuroscience (NLTN) "Neurodevelopmental disorders" "Adult nervous system disorders" (RRF-2.3.1-21-2022-00011), K137607 and K129049. This research was supported by the ÚNKP-21-4-SZTE-127 New National Excellence Program of the Ministry for Innovation and Technology from the source of the National Research, Development and Innovation Fund (Sz. D.). We gratefully acknowledge Prof. Árpád Molnár for language proofreading.

Appendix A. Supplementary data

Supplementary data to this article can be found online at https://doi.org/10.1016/j.taap.2023.116548.

References

Angerer, V., Mogler, L., Steitz, J.P., Bisel, P., Hess, C., Schoeder, C.T., Müller, C.E., Huppertz, L.M., Westphal, F., Schäper, J., Auwärter, V., 2018. Structural characterization and pharmacological evaluation of the new synthetic cannabinoid CUMYL-PEGACLONE. Drug Test. Anal. 10 (3), 597–603. https://doi.org/10.1002/dta.2237.

Banister, S.D., Longworth, M., Kevin, R., Sachdev, S., Santiago, M., Stuart, J., Mack, J.B. C., Glass, M., McGregor, I.S., Connor, M., Kassiou, M., 2016. Pharmacology of Valinate and tert-Leucinate synthetic cannabinoids 5F-AMBICA, 5F-AMB, 5F- ADB, AMB-FUBINACA, MDMB-FUBINACA, MDMB-CHMICA, and their analogues. ACS Chem. Neurosci. 7 (9), 1241–1254. https://doi.org/10.1021/acschemneuro.6b00137.

Besli, G.E., Ikiz, M.A., Yildirim, S., Saltik, S., 2015. Synthetic cannabinoid abuse in adolescents: a case series. J. Emerg. Med. 49 (5), 644–650. https://doi.org/10.1016/j.jemermed.2015.06.053.

Brandt, S.D., 2019. Critical Review Report: 5F-MDMB-PICA. Technical Report, World Health Organisation, Geneva, Switzerland. https://researchonline.ljmu.ac.uk/id/eprint/11446/1/ECDD42_5F-MDMB-PICA.pdf (accessed October 3. 2019, last modified October 29. 2021).

Cabanlong, C.V., Russell, L.N., Fantegrossi, W.E., Prather, P.L., 2022. Metabolites of synthetic cannabinoid 5F-MDMB-PINACA retain affinity, act as high efficacy agonists and exhibit atypical pharmacodynamic properties at CB1 receptors. Toxicol. Sci. 187 (1), 175–185. https://doi.org/10.1093/toxsci/kfac024.

Cannaert, A., Sparkes, E., Pike, E., Luo, J.L., Fang, A., Kevin, R.C., Ellison, R., Gerona, R., Banister, S.D., Stove, C.P., 2020. Synthesis and in vitro cannabinoid receptor 1 activity of recently detected synthetic cannabinoids 4F-MDMB-BICA, 5F-MPP-PICA, MMB-4en-PICA, CUMYL-CBMICA, ADB-BINACA, APP-BINACA, 4F-MDMB-BINACA, MDMB-4en-PINACA, A-CHMINACA, 5F-AB-P7AICA, 5F-MDMB-P7AICA, and 5F-AP7AICA. ACS Chem. Neurosci. 11 (24), 4434–4446. https://doi.org/10.1021/acschemneuro.0c00644.

Dimmito, M.P., Stefanucci, A., Pieretti, S., Minosi, P., Dvorácskó, S., Tömböly, C., Zengin, G., Mollica, A., 2019. Discovery of orexant and anorexant agents with indazole scaffold endowed with peripheral antiedema activity. Biomolecules 9 (9), 492. https://doi.org/10.3390/biom9090492.

Dvorácskó, S., Keresztes, A., Mollica, A., Stefanucci, A., Macedonio, G., Pieretti, S., Zádor, F., Walter, F.R., Deli, M.A., Kékesi, G., Bánki, L., Tuboly, G., Horváth, G., Tömböly, C., 2019. Preparation of bivalent agonists for targeting the mu opioid and cannabinoid receptors. Eur. J. Med. Chem. 178, 571–588. https://doi.org/10.1016/j.ejmech.2019.05.037.

Dvorácskó, S., Lázár, L., Fülöp, F., Palkó, M., Zalán, Z., Penke, B., Fülöp, L., Tömböly, C., Bogár, F., 2021. Novel high affinity sigma-1 receptor ligands from minimal ensemble docking-based virtual screening. Int. J. Mol. Sci. 2021 (22), 8112. https://doi.org/10.3390/ijms22158112.

EMCDDA, 2020. EMCDDA Initial Report on the New Psychoactive Substance 4F-MDMB-BICA, Lisbon. https://www.emcdda.europa.eu/system/files/publications/13362/emcdda-initial-report-4F-MDMB-BICA.pdf (accessed November 2020).

Giorgetti, A., Barone, R., Pelletti, G., Garagnani, M., Pascali, J., Haschimi, B., Auwärter, V., 2022. Development and validation of a rapid LC-MS/MS method for the detection of 182 novel psychoactive substances in whole blood. Drug Test. Anal. 14 (2), 202–223. https://doi.org/10.1002/dta.3170.

Hutton, F., 2022. The co-production of shifting intoxications: synthetic cannabinoids, stigma, risk and harm. Drugs (Abingdon Engl). 1-11 https://doi.org/10.1080/09687637.2022.2042486.

Institóris, L., Kovács, K., Sija, É., Berkecz, R., Körmöczi, T., Németh, I., Elek, I., Bakos, Á., Urbán, I., Pap, C., Kereszty, É., 2022a. Clinical symptoms and blood concentration of new psychoactive substances (NPS) in intoxicated and hospitalized patients in the Budapest region of Hungary (2018-19). Clin. Toxicol. 60 (1), 18–24. https://doi.org/10.1080/15563650.2021.1928162.

Institóris, L., Hidvégi, E., Kovács, K., Jámbor, Á., Dobos, A., Rárosi, F., Süvegh, G., Varga, T., Kereszty, É.M., 2022b. Drug consumption of suspected drug-influenced drivers in Hungary (2016–2018). Forensic Sci. Int. 336, 111325 https://doi.org/10.1016/j.forsciint.2022.111325.

Iudici, A., Castelnuovo, G., Faccio, E., 2015. New drugs and polydrug use: implications for clinical psychology. Front. Psychol. 6, 267. https://doi.org/10.3389/fpsyg.2015.00267.

Janssens, L.K., Hudson, S., Wood, D.M., Wolfe, C., Dargan, P.I., Stove, C.P., 2022. Linking in vitro and ex vivo CB1 activity with serum concentrations and clinical features in 5F-MDMB-PICA users to better understand SCRAs and their metabolites. Arch. Toxicol. 96 (11), 2935–2945. https://doi.org/10.1007/s00204-022-03355-6.

Kleis, J., Germerott, T., Halter, S., Héroux, V., Roehrich, J., Schwarz, C.S., Hess, C., 2020. The synthetic cannabinoid 5F-MDMB-PICA: A case series. Forensic Sci. Int. 314, 110410 https://doi.org/10.1016/j.forsciint.2020.110410.

Kleis, J.N., Hess, C., Germerott, T., Roehrich, J., 2021. Sensitive screening of synthetic cannabinoids using liquid chromatography quadrupole time-of-flight mass spectrometry after solid phase extraction. Drug Test. Anal. 13 (8), 1535–1551. https://doi.org/10.1002/dta.3052.

Körmöczi, T., Sija, É., Institóris, L., Kereszty, É.M., Ilisz, I., Berkecz, R., 2022. Analytical methodologies for the characterization and analysis of the parent compound and phase I metabolites of 4F-MDMB-BICA in human microsome, urine and blood samples. J. Anal. Toxicol. 46 (2), 135–145. https://doi.org/10.1093/jat/bkab004.

Krishnamurthy, S., Kadu, R.D., 2023. A comprehensive review on detection of cannabinoids using hyphenated techniques. Chem. Pap. 1-20 https://doi.org/10.1007/s11696-023-02732-4.

Krotulski, A.K., Garibay, N., Walther, D., Walton, S.E., Mohr, A.L.A., Logan, B.K., Baumann, M.H., 2021. Pharmacokinetics and pharmacodynamics of the synthetic cannabinoid, 5F-MDMB-PICA, in male rats. Neuropharmacology. 199, 108800 https://doi.org/10.1016/j.neuropharm.2021.108800.

Lie, W., Cheong, E.J.Y., Goh, E.M.L., Moy, H.Y., Cannaert, A., Stove, C.P., Chan, E.C.Y., 2021. Diagnosing intake and rationalizing toxicities associated with 5F-MDMB-PINACA and 4F-MDMB-BINACA abuse. Arch. Toxicol. 95 (2), 489–508. https://doi.org/10.1007/s00204-020-02948-3.

Luethi, D., Liechti, M.E., 2020. Designer drugs: mechanism of action and adverse effects. Arch. Toxicol. 94, 1085–1133. https://doi.org/10.1007/s00204-020-02693-7.

Mogler, L., Franz, F., Rentsch, D., Angerer, V., Weinfurtner, G., Longworth, M., Banister, S.D., Kassiou, M., Moosmann, B., Auwärter, V., 2018. Detection of the recently emerged synthetic cannabinoid 5F–MDMB-PICA in 'legal high'products and human urine samples. Drug Test. Anal. 10, 196–205. https://doi.org/10.1002/dta.2201.

Mollica, A., Pelliccia, S., Famiglini, V., Stefanucci, A., Macedonio, G., Chiavaroli, A., Orlando, G., Brunetti, L., Ferrante, C., Pieretti, S., Novellino, E., Benyhe, S., Zador, F., Erdei, A., Szucs, E., Samavati, E., Dvoracsko, S., Tomboly, C., Ragno, R., Patsilinakos, A., Silvestri, R., 2017. Exploring the first Rimonabant analog-opioid peptide hybrid compound, as bivalent ligand for CB1 and opioid receptors. J. Enzym. Inhib. Med. Chem. 32, 444–451. https://doi.org/10.1080/14756366.2016.1260565.

Musa, A., Simola, N., Piras, G., Caria, F., Onaivi, E.S., De Luca, M.A., 2020. Neurochemical and behavioral characterization after acute and repeated exposure to novel synthetic cannabinoid agonist 5-MDMB-PICA. Brain Sci. 10 (12), 1011. https://doi.org/10.3390/brainsci10121011.

Noble, C., Cannaert, A., Linnet, K., Stove, C.P., 2019. Application of an activity-based receptor bioassay to investigate the in vitro activity of selected indole- and indazole-3-carboxamide-based synthetic cannabinoids at CB1 and CB2 receptors. Drug Test. Anal. 11, 501–511. https://doi.org/10.1002/dta.2517.

Potts, A.J., Cano, C., Thomas, S.H.L., Hill, S.L., 2020. Synthetic cannabinoid receptor agonists: classification and nomenclature. Clin. Toxicol. 58, 82–98. https://doi.org/10.1080/15563650.2019.1661425.

Qin, S., Xin, G., Wei, J., He, G., Yuan, Z., Liu, H., Zhang, X., Wang, Y., Zhang, W., Lu, J., 2022. Metabolic profiles of 5F-MDMB-PICA in human urine, serum and hair samples using LC–Q exactive HF-MS. J. Anal. Toxicol. 46 (4), 408–420. https://doi.org/10.1093/jat/bkab034.

Risseeuw, M.D., Blanckaert, P., Coopman, V., Van Quekelberghe, S., Van Calenbergh, S., Cordonnier, J., 2017. Identification of a new tert-leucinate class synthetic cannabinoid in powder and "spice-like" herbal incenses: methyl 2-[[1-(5-fluoro-pentyl) indole-3-carbonyl] amino]-3, 3-dimethyl-butanoate (5F-MDMB-PICA). Forensic Sci. Int. 273, 45–52. https://doi.org/10.1016/j.forsciint.2017.01.023.

Shi, Y., Zhou, L., Li, L., Liu, M., Qiang, H., Shen, M., Shen, B., Chen, H., Drummer, O.H., Liu, W., Wu, H., Xiang, P., 2020. Detection of a new tert-leucinate synthetic cannabinoid 5F-MDMB-PICA and its metabolites in human hair: application to authentic cases. Front. Chem. 8, 1124. https://doi.org/10.3389/fchem.2020.610312.

Sim, L.J., Selley, D.E., Childers, S.R., 1995. In vitro autoradiography of receptor-activated g proteins in rat brain by agonist-stimulated guanylyl 5′-Gamma-[35S] thiol-triphosphate binding. Proc. Natl. Acad. Sci. U. S. A. 92 (16), 7242–7246. https://doi.org/10.1073/pnas.92.16.7242.

Stefanucci, A., Macedonio, G., Dvorácskó, S., Tömböly, C., Mollica, A., 2018. Novel Fubinaca/Rimonabant hybrids as endocannabinoid system modulators. Amino Acids 50, 1595–1605. https://doi.org/10.1007/s00726-018-2636-1.

Szpot, A., Nowak, K., Wachełko, O., Tusiewicz, K., Chłopaś-Konowałek, A., Zawadzki, M., 2022. Methyl (S)-2-(1–7 (5-fluoropentyl)-1H-indole-3-carboxamido)-3,3-dimethylbutanoate (5F-MDMB-PICA) intoxication in a child with identification of two new metabolites (ultra-high-performance liquid chromatography–tandem mass spectrometry). Forensic. Toxicol. 41, 47–58. https://doi.org/10.1007/s11419-022-00629-7.

Tokarczyk, B., Jurczyk, A., Krupińska, J., Adamowicz, P., 2022. Fatal intoxication with new synthetic cannabinoids 5F-MDMB-PICA and 4F-MDMB-BINACA—parent compounds and metabolite identification in blood, urine and cerebrospinal fluid. Forensic. Sci. Med. Pathol. 1-10 https://doi.org/10.1007/s12024-022-00492-3.

Truver, M.T., Watanabe, S., Åstrand, A., Vikingsson, S., Green, H., Swortwood, M.J., Kronstrand, R., 2020. 5F-MDMB-PICA metabolite identification and cannabi- noid receptor activity. Drug Test. Anal. 12, 127–135. https://doi.org/10.1002/dta.2688.

Wagner, K.D., Armenta, R.F., Roth, A.M., Maxwell, J.C., Cuevas-Mota, J., Garfein, R.S., 2014. Use of synthetic cathinones and cannabimimetics among injection drug users in San Diego, California. Drug Alcohol Depend. 141, 99–106. https://doi.org/10.1016/j.drugalcdep.2014.05.007.

WHO, 2019. World Health Organization, Critical review report: 5F-MDMB-PICA; Expert committee on drug dependence, 42nd Meeting. Geneva, World Health Organization 2019 Oct 21- 25. https://researchonline.ljmu.ac.uk/id/eprint/11446/1/ECDD42_5F-MDMB-PICA.pdf (accessed 21-25 October 2019).

Wu, J., Zhang, F., Ke, X., Jia, W., Wan, X., Zhang, L., Fan, Y., Zhou, J., 2023. Rapid simultaneous determination of 11 synthetic cannabinoids in urine by liquid chromatography-triple quadrupole mass spectrometry. Separations 10 (3), 203. https://doi.org/10.3390/separations10030203.

Zádor, F., Nagy-Grócz, G., Dvorácskó, S., Bohár, Z., Cseh, E.K., Zádori, D., Párdutz, Á., Szűcs, E., Tömböly, C., Borsodi, A., Benyhe, S., Vécsei, L., 2020. Long-term systemic administration of kynurenic acid brain region specifically elevates the abundance of functional CB1 receptors in rats. Neurochem. Int. 138, 104752 https://doi.org/10.1016/j.neuint.2020.104752.